Journal of Applied Polymer Science

Synthesis of Azobenzene-Containing Side Chain Liquid Crystalline Diblock Copolymers Using RAFT Polymerization and Photo-Responsive Behavior

Wuqiong Sun,[1] Xiaohua He,[1] Xiaojuan Liao,[1] Shaoliang Lin,[2] Wei Huang,[1] Meiran Xie[1]

[1]Department of Chemistry, East China Normal University, 500 Dongchuan Road, Shanghai 200241, China

[2]Shanghai Key Laboratory of Advanced Polymer Materials, School of Materials Science and Engineering, East China University of Science and Technology, Shanghai 200237, China

Correspondence to: X. He (E-mail: xhhe@chem.ecnu.edu.cn); S. Lin (E-mail: slin@ecust.edu.cn)

ABSTRACT: Well-defined azobenzene-containing side chain liquid crystalline diblock copolymers composed of poly[6-[4-(4-methoxyphenylazo)phenoxy]hexyl methacrylate] (PAzoMA) and poly(glycidyl methacrylate) (PGMA) were synthesized by a two-step reversible addition–fragmentation chain transfer polymerization (RAFT). The thermal liquid-crystalline phase behavior of the PGMA-*b*-PAzoMA diblock copolymers in bulk were measured by differential scanning calorimetry (DSC) and polarized light microscopy (POM). The synthesized diblock copolymers exhibited a smectic and nematic liquid crystalline phase over a relatively wide temperature range. With increasing the weight fraction of the PAzoMA block, the phase transition temperatures, and corresponding enthalpy changes increased. Atomic force microscope (AFM) measurements confirmed the formation of the microphase separation in PGMA-*b*-PAzoMA diblock copolymer thin films and the microphase separation became more obvious after cross-linking the PGMA block. The photochemical transition behavior of the PGMA-*b*-PAzoMA diblock copolymers in solution and in thin films were investigated by UV–vis spectrometry. It was found that the *trans–cis* isomerization of diblock copolymers was slower than that of the corresponding PAzoMA homopolymer and the photoisomerization rates decreased with increasing either the length of PAzoMA block or PGMA block. The photo-induced isomerization in solid films was quite different with that in $CHCl_3$ solution due to the aggregation of the azobenzene chromophore. The cross-linking structures severely suppressed the photoisomerization of azobenzene chromophore. These results may provide guidelines for the design of effective photo-responsive anisotropic materials. © 2013 Wiley Periodicals, Inc. J. Appl. Polym. Sci. 000: 000–000, 2013

KEYWORDS: copolymers; liquid crystals; films

Received 6 February 2013; accepted 14 April 2013; Published online
DOI: 10.1002/app.39407

INTRODUCTION

In recent years, much effort has been devoted to azobenzene-containing polymers (azo polymers for short) due to their interesting properties related to the reversible photoisomerization between the stretched *trans* and the bent *cis* isomers of the chromophores.[1–4] Azobenzene-containing side-chain liquid crystalline polymers (Azo-SCLCPs for short), are one of the most interesting azo polymer materials due to the combination of the liquid crystalline anisotropy and the photo-induced isomerization, in which azobenzene moieties play roles as both mesogens and photosensitive chromophores. Especially, incorporation of Azo-SCLCPs segments into block copolymers has been extensively studied from both academic and industrial point of views because they can form different microphase-segregated nanostructures such as spheres, cylinders, gyroids, and lamellae,[5,6] and the well-ordered nanostructures can greatly affect the photoisomerization of the azobenzene chromophores. At the same time, the photo-responsive azobenzene chromophores which undergo reversible *trans–cis* isomerization upon photo irradiation can act as a probe to study the relationships between the photoisomerization, the microphase separation, and the microdomain nanostructures.[7–17] To further explore the relationships between structures and properties, the synthesis of well-defined model block copolymers containing Azo-SCLCPs and different chemical structure segments are much desired.

Reversible addition–fragmentation chain transfer polymerization (RAFT) offers a powerful tool of the polymerization for the controlled manipulation of macromolecular architecture due to

Additional Supporting Information may be found in the online version of this article.

Applied Polymer SCIENCE

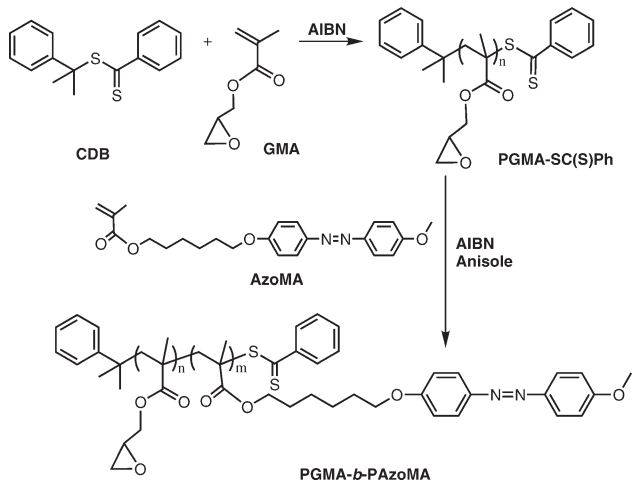

Scheme 1. Synthesis of diblock copolymer PGMA-*b*-PAzoMA. CDB = cumyl dithiobenzoate; GMA = glycidyl methacrylate; AIBN = 2,2′-azobis(isobutyronitrile); PGMA = poly(glycidyl methacrylate); AzoMA = 6-[4-(4-methoxyphenylazo)phenoxy]hexyl methacrylate; PAzoMA = poly{6-[4-(4-methoxyphenylazo)phenoxy]hexyl methacrylate}.

polymerization of a wide variety of monomers, tolerance of a wide range of functional groups, and very facile preparation of block copolymers with a narrow polydispersity index.[18] Meanwhile, there is no impurities or residual reagents [e.g., atom transfer radical polymerization (ATRP) metal ions, dipyridyl, etc.] to remove from the polymerization product and the reaction temperature is relatively lower, usually between 60–70°C. With the availability of RAFT, there have been more and more reports about the synthesis of block copolymers composed of azo polymer and other segment.[1516–30] For example, Zhao et al.[24] reported the synthesis of a new type of double side-chain liquid crystalline polymers composed of poly{6-[4-(4-methoxyphenylazo)phenoxy]hexyl methacrylate} and poly{6-[4-(4-cyanophenyl)phenoxy]hexyl methacrylate} (PAzoMA-*b*-PBiPMA) by RAFT using 2-(2-cyanopropyl)dithiobenzoate (CPDB) as RAFT agent and AIBN as initiator. The obtained results verified the photo-induced orientation of azobenzene mesogens of PAzoMA could propagate into the microphase-segregated PBiPMA domains through the interface, resulting in an orientation of the biphenyl mesogens of PBiPMA in the same direction. Recently, they also employed RAFT method to synthesize amphiphilic azobenzene-containing side-chain liquid crystalline block copolymers with the hydrophilic block either poly(acrylic acid) (PAA) or poly(*N,N*-dimethylacrylamide) (PDMA), which could form large vesicles in aqueous solution with a side-chain liquid crystalline polymer (SCLCP) membrane.[28] This study showed that a photo-induced liquid crystalline order–disorder transition could occur inside the vesicle membrane in aqueous solution. Of course, RAFT method has been also employed to synthesize other block copolymers composed of SCLCP and other segment.[31]

This article reports that the synthesis of a series of novel side-chain liquid crystalline diblock copolymers based on poly(glycidyl methacrylate) (PGMA) and poly(6-[4-(4-methoxyphenylazo)phenoxy]hexyl methacrylate) (PAzoMA) via a two-step RAFT polymerization, using cumyl dithiobenzoate (CDB) as the initial RAFT agent and AIBN as initiator. PGMA was chosen as the coil segment and the epoxy groups can be cross-linked with diamines at high temperature. The use of PAzoMA renders this block copolymer photoactive and enables us to investigate the effect of the cross-linking structure and microphase separation on photo-responsive property in this new type of block copolymer. The synthesis of PGMA-*b*-PAzoMA is shown in Scheme 1.

EXPERIMENTAL

Materials

The monomers, glycidyl methacrylate (GMA, 97%; Shanghai Jingchun Reagent Co., China) was passed through inhibitor removing columns before use, 6-[4-(4-methoxyphenylazo)phenoxy]hexyl methacrylate (AzoMA) was synthesized according to the procedure reported by Stewart and Imrie.[32] The initiator 2,2′-azobis(isobutyronitrile) (AIBN, 97%) was recrystallized twice in methanol and stored at 4°C. The RAFT agent cumyl dithiobenzoate (CDB) was synthesized according to literature procedures,[33] and the full synthesis and purification procedures were detailed in Supporting Information. Anisole (A.R. grade) was purified by washing with 10% NaOH three times, followed by washing twice with deionized water, dried with $CaCl_2$, and then distilled over CaH_2 under reduced pressure. *N,N*-Dimethyl formamide (DMF; A.R. grade) was dried with 4 Å molecular sieves and distilled under vacuum. Other reagents (A.R. grade) were purchased from Shanghai Chemical Reagent Company and used as received.

Synthesis of Poly(glycidyl methacrylate) Capped with Dithiobenzoate [PGMA-SC(S)Ph]

The macromolecular RAFT agent PGMA–SC(S)Ph was synthesized by a typical RAFT polymerization according to the literature.[34] A Schlenk tube was charged with degassed GMA (4.3 g, 0.03 mol), AIBN (24.6 mg, 0.15 mmol), CDB (0.2 g, 0.73 mmol), and a magnetic stirrer. The purplish red mixture was purged with dry nitrogen and subjected to three freeze–pump–thaw cycles to remove any dissolved oxygen. Then the tube was sealed under vacuum and immersed in an oil bath at 65°C for 6 h. The reaction was stopped and the tube was quickly cooled down to the room temperature with cold water. The mixture was diluted with THF and precipitated into excess cold methanol. The product was purified by reprecipitating three times from THF to cold methanol and dried in vacuum at room temperature overnight. PGMA–SC(S)Ph was obtained as a pink powder. Yield: 2.7 g (60%). $M_{n,GPC}$ = 5 840 g mol^{-1}, M_w/M_n = 1.23, degree of polymerization (DP; ^{1}H NMR = 42). Thus, the obtained product was denoted as $PGMA_{42}$–SC(S)Ph. According to a similar method, another macromolecular RAFT agent $PGMA_{65}$–SC(S)Ph was also prepared ($M_{n,GPC}$ = 8 560 g mol^{-1}, M_w/M_n = 1.22).

Synthesis of Homopolymer PAzoMA

A Schlenk tube was charged with AzoMA (3.1 g, 7.8 mmol), AIBN (4.92 mg, 0.03 mmol), CDB (0.03 g, 0.12 mmol), 3.5 mL anhydrous anisole, and a magnetic stirrer. The orange-yellow mixture was purged with dry nitrogen and subjected to three freeze–pump–thaw cycles to remove any dissolved oxygen. Then the tube was sealed under vacuum and immersed in an oil bath

Table I. Characterization of the Synthesized Polymers

Polymer[a]	Yield (%)	M_n[b] (g mol^{-1})	PDI[b]	f_{PAzoMA}[c] (wt %)
$PGMA_{42}$	60	5840	1.23	-
$PGMA_{65}$	62	8560	1.22	-
$PAzoMA_{60}$	85	18,300	1.17	100
$PGMA_{42}$-*b*-$PAzoMA_{22}$	85	11,500	1.21	60
$PGMA_{42}$-*b*-$PAzoMA_{39}$	86	15,600	1.22	72
$PGMA_{42}$-*b*-$PAzoMA_{63}$	80	20,500	1.21	81
$PGMA_{65}$-*b*-$PAzoMA_{28}$	86	17,900	1.20	54
$PGMA_{65}$-*b*-$PAzoMA_{38}$	84	20,400	1.23	62
$PGMA_{65}$-*b*-$PAzoMA_{67}$	85	25,000	1.25	74

[a] Determined by ^{1}H NMR.

[b] Determined by GPC in THF with calibrated PS standards at 35°C.

[c] The wt % content was determined by ^{1}H NMR.

at 75°C for 12 h. The reaction was stopped and the tube was quickly cooled down to the room temperature with cold water. The mixture was diluted with THF and precipitated into excess diethyl ether. The product was purified by reprecipitating three times from THF to diethyl ether, dried in vacuum at room temperature overnight and obtained as a yellow powder. Yield: 2.6 g (85%). $M_{n,GPC}$=1.83 × 10^4 g mol^{-1}, M_w/M_n = 1.17, DP ^{1}H NMR = 60. Thus, the obtained product was denoted as $PAzoMA_{60}$.

Synthesis of Diblock Copolymer PGMA-b-PAzoMA

The target diblock copolymer PGMA-*b*-PAzoMA was synthesized via a similar method reported for the RAFT polymerization of monomers containing azobenzene side groups.[19] The typical experiment was as follows: AzoMA (0.5 g, 1.3 mmol), AIBN (3.0 mg, 0.018 mmol), $PGMA_{42}$–SC(S)Ph (0.3 g, 0.048 mmol), and 3 mL anhydrous anisole were added in a Schlenk tube. After degassing with three freeze–pump–thaw cycles, the tube was sealed under vacuum and immersed into an oil bath at 75°C for 12 h. The mixture was diluted with THF and then dropped into diethyl ether. The product was purified by reprecipitating three times from THF to cold diethyl ether and dried in a vacuum oven at room temperature overnight. PGMA-*b*-PAzoMA was obtained as a yellow powder. Yield: 0.7 g (85%). $M_{n,GPC}$ = 1.15 × 10^4 g mol^{-1}, M_w/M_n = 1.21. DP (^{1}H NMR) = 22. Thus, the obtained product was denoted as $PGMA_{42}$-*b*-$PAzoMA_{22}$. According to a similar method, other AB diblock copolymers were also synthesized under the same polymerization time and temperature. Table I summarized the molecular characteristics of the PGMA homopolymers and PGMA-*b*-PAzoMA diblock copolymers presented in this study.

Sample Preparation

The PGMA-*b*-PAzoMA diblock copolymers were dissolved in $CHCl_3$ at 2.0 × 10^{-2} g L^{-1} and filtered through a N6 filter (0.45 μm) for the measurement of the photo-responsive behavior of the polymer solution.

Polymer films with a thickness of about 200 nm were prepared by spin-coating the diblock copolymer toluene solutions (~3 wt %) on silicon wafers. The as-coated films were dried at 40°C in a vacuum oven over night. The annealed films were prepared by thermal treatment at 140°C (a little higher than the nematic-to-isotropic transition temperature, T_{NI}) in vacuum for 2 h, followed by subsequent cooling down to the room temperature at a rate of 5°C min^{-1}. For the cross-linked films, hexane diamine (molar ratio to epoxy groups in the diblock copolymer = 1 : 2) was added to the diblock copolymer toluene solutions (~3 wt %) and stirred overnight to get a mixed homogeneous solution. Then the mixed solution was spin-coated on silicon wafers and cured at 120°C for 3 h in a vacuum oven. The cross-linked films were no longer dissolved in toluene and DMF (which are good solvent for the PGMA-*b*-PAzoMA diblock copolymers).

Instruments and Measurements

Molecular weights M_n and polydispersity M_w/M_n were determined by gel permeation chromatography (Waters 150C) equipped with three Waters Styragel columns (10^3, 10^4, and 10^5 Å) and refractive index detector (set at 35°C), using THF as the eluent at a flow rate of 1.0 mL min^{-1} at 35°C. The column system was calibrated by a series of monodispersed polystyrene standards. ^{1}H NMR spectra were recorded on a 500 Hz NMR instrument spectrometer. $CDCl_3$ was used as solvent and TMS was used as a reference for chemical shifts. FT-IR spectra were recorded on a Perkin-Elmer Spectrum One spectrometer at frequencies ranging from 400 to 4000 cm^{-1} using KBr pellet method. The differential scanning calorimetry (DSC) analysis was carried out on a Perkin-Elmer Pyris-1 instrument under nitrogen flow from −10°C to 160°C with a heating or cooling rate of 10°C min^{-1}. The polarized optical microscopy images used to analyze the thermal transitions and observe liquid crystalline textures were recorded on a Leica DMLP Polarized optical microscope (POM) with a Leitz 350 hot stage. The photo-isomerization of the azo chromophores was induced by irradiation with a high-intensity lamp (Uvata UP115). The light intensity was 150 mW/cm^2 at 365 nm and 300 mW/cm^2 at 450 nm. The UV–vis spectra of the samples were measured over different irradiation time intervals by using a Jasco V-50 spectrophotometer at 25°C. The atomic force microscopy images of block copolymer thin films were taken on a Veeco Nanoscope IIIa Multimode AFM microscope at 25°C in tapping mode.

RESULTS AND DISCUSSION

Synthesis of PGMA-b-PAzoMA Diblock Copolymers by RAFT

RAFT polymerization is a facial, versatile, and efficient technique to prepare block copolymers with well-defined architectures and predesigned molecular weights. It can be applied to a wide variety of functional monomers and the purification is much more easily than that of atom transfer radical polymerization (ATRP).[18] In our research, CDB was first used as a chain transfer agent (CTA) for the RAFT polymerization of GMA monomer to obtain PGMA homopolymer capped with dithiobenzoate. Then PGMA homopolymer was used as a macro-RAFT agent for the second-step RAFT polymerization of AzoMA monomer. The synthetic route is shown in Scheme 1. The structures of the PGMA macro-RAFT agents and corresponding diblock copolymers PGMA-*b*-PAzoMA were characterized by GPC, FT-IR, and ^{1}H NMR spectroscopy.

Applied Polymer SCIENCE

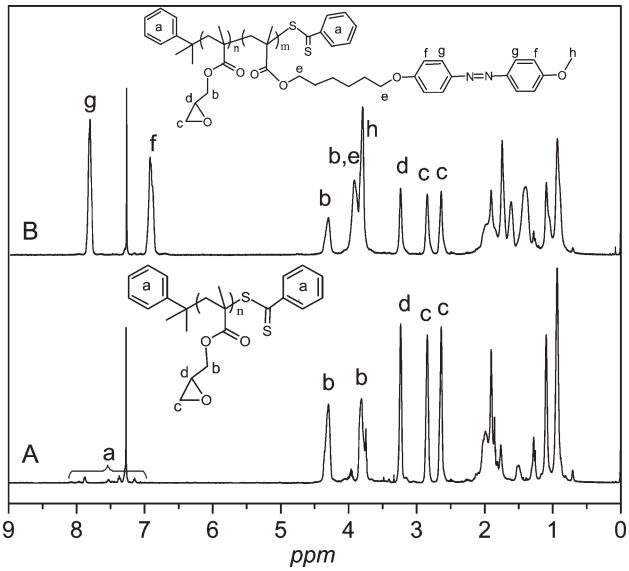

Figure 1. ^{1}H NMR spectra of (A) PGMA–SC(S)Ph and (B)PGMA-*b*-PAzoMA in $CDCl_3$.

The macro-RAFT agent PGMA–SC(S)Ph was synthesized by the RAFT polymerization using CDB as the RAFT agent and AIBN as the initiator in bulk at 65°C, according to the literature.[34] The typical ^{1}H NMR spectrum of PGMA–SC(S)Ph recorded in $CDCl_3$ is shown in Figure 1(A). The resonance signals originating from the phenyl end groups, which are derived from the RAFT agent CDB, can be clearly observed between 7.10 and 7.90 ppm [Figure 1(A: a)]. The chemical shifts at 3.81 and 4.30 ppm are assigned to the methylene (–OC***H***$_2$–) [Figure 1(A: b)] adjacent to the epoxy groups and the peaks at 2.63, 2.84, and 3.24 ppm [Figure 1(A: c and d)] are attributed to methylene and methine of the epoxy side groups. The resonance signals related to the methacrylate backbone can also be found between 0.66 and 2.21 ppm in Figure 1(A). The degree of polymerization (DP) of the PGMA–SC(S)Ph can be controlled by the molar ratio of GMA monomer to CDB RAFT agent, and its value is calculated by the integral ratio of methylene protons adjacent to the epoxy side groups of PGMA–SC(S)Ph [Figure 1(A: b)] to the phenyl end groups derived from CDB [Figure 1(A: a)]. Two samples were prepared by altering the monomer-to-RAFT agent molar ratio. The two PGMA–SC(S)Ph macro-RAFT agents are denoted as $PGMA_{42}$–SC(S)Ph and $PGMA_{65}$–SC(S)Ph. On the other hand, the characteristic absorptions at 1720 and 905 cm^{-1} attributed to C=O ester groups and epoxy groups, respectively, can be clearly observed in the FT-IR spectrum of PGMA–SC(S)Ph, as shown in Figure 2(A). The molecular weights and polydispersity index (PDI) of the PGMA–SC(S)Ph macro-RAFT agents were tested by GPC using THF as eluent and a set of mono-dispersed PS as the standard. The relevant data are listed in Table I. It is suggested that the two PGMA–SC(S)Ph samples had narrow molecular weight distributions (PDI = 1.23 and 1.22) and molecular weights increased from 5840 to 8560 g mol^{-1}. The results obtained from ^{1}H NMR, FT-IR, and GPC measurements confirmed that PGMA–SC(S)Ph macro-RAFT agents had been successfully prepared by RAFT polymerization.

The diblock copolymers PGMA-*b*-PAzoMA were prepared by RAFT polymerization using PGMA–SC(S)Ph as the macro-RAFT agent and AIBN as the initiator in anisole at 75°C, following a typical method described before.[19] Figure 1(B) exhibits a representative ^{1}H NMR spectrum of PGMA-*b*-PAzoMA diblock copolymers in $CDCl_3$. The proton signals of the CDB residual units cannot be clearly observed and partially overlapped with the phenyl groups of the PAzoMA block. The chemical shifts at 2.63, 2.84, and 3.23 ppm are located to methylene and methine of the epoxy side groups from PGMA segment [Figure 1(B: c and d)]. One of the two proton peaks assigned to the methylene [–OC***H***$_2$–; Figure 1(B: b)] adjacent to the epoxy groups appeared at 4.30 ppm, the other was overlapped with PAzoMA block [Figure 1(B: e)]. The protons signals at 7.81 and 6.91 ppm are assigned to the phenyl groups [Figure 1(B: g and f)] originating from the azobenzene moieties of the PAzoMA block. The resonance signals of the protons of methylene groups adjacent to the oxygen atom [Figure 1(B: e)] and methoxyl group [Figure 1(B: h)] of PAzoMA block can be found at 3.92 and 3.80 ppm, respectively, and were partially overlapped with each other. The DP of the PAzoMA block can be controlled by the molar ratio of AzoMA monomer to PGMA–SC(S)Ph macro-RAFT agent, and its value can be calculated by the integral ratio of the phenyl moiety of azobenzene side groups of PAzoMA segment [Figure 1(B: g and f)] at 7.81 or 6.91 ppm to the methylene and methine of the epoxy side groups from PGMA segment at 2.63, 2.84, and 3.23 ppm [Figure 1(B: c and d)]. Thus, the diblock copolymers PGMA-*b*-PAzoMA are denoted as $PGMA_{42}$-*b*-$PAzoMA_n$ (n = 22, 39, and 63) and $PGMA_{65}$-*b*-$PAzoMA_m$ (m = 28, 38, and 67). The FT-IR spectrum of PGMA-*b*-PAzoMA diblock copolymers [Figure 2(B)] shows not only the characteristic absorptions at 905 cm^{-1} assigned to the epoxy groups of the PGMA block but also that of the 1600 cm^{-1} assigned to the phenyl groups of the PAzoMA block, and the absorption at 1720 cm^{-1} is attributed to the C=O ester groups of both PGMA and PAzoMA segments. The

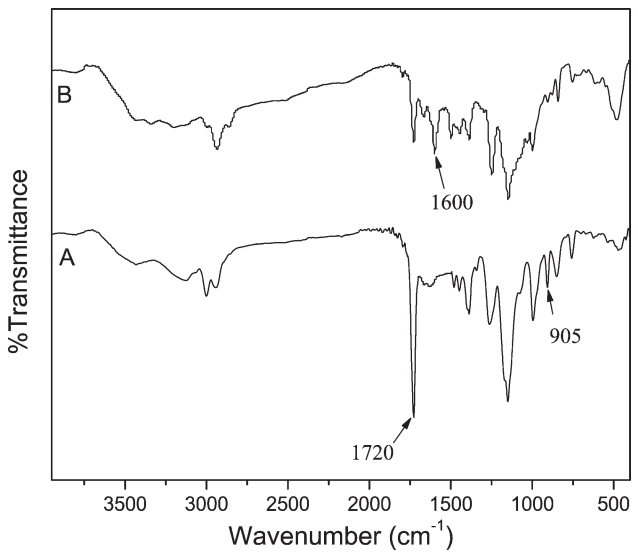

Figure 2. FT-IR spectra of (A) PGMA–SC(S)Ph and (B) PGMA-*b*-PAzoMA.

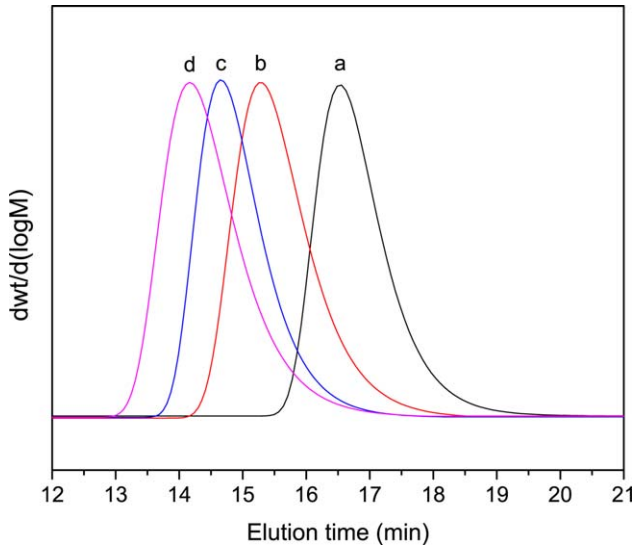

Figure 3. GPC traces of (a) $PGMA_{42}$–SC(S)Ph, (b) $PGMA_{42}$-*b*-$PAzoMA_{22}$, (c) $PGMA_{42}$-*b*-$PAzoMA_{39}$, and (d) $PGMA_{42}$-*b*-$PAzoMA_{63}$. [Color figure can be viewed in the online issue, which is available at wileyonlinelibrary.com.]

molecular weights and PDI of PGMA-*b*-PAzoMA diblock copolymers were tested by GPC. The results are also listed in Table I and the GPC curves of $PGMA_{42}$-*b*-$PAzoMA_n$ (n = 22, 39, and 63) series are displayed in Figure 3. All of the samples show unimodal peaks with narrow molecular weight distributions (PDI = 1.20–1.25) and the molecular weights increase with increasing the degree of polymerization. These obtained results verified that the diblock copolymers PGMA-*b*-PAzoMA had been successfully synthesized via a two-step RAFT polymerization. The novel diblock copolymers can be used as a coil-rod modal block copolymer for the research of the morphological structures and photo-responsive behavior.

Thermotropic Phase Behavior

A combination of differential scanning calorimetry (DSC) and polarized microscopy (POM) measurements was carried out to study the thermal properties and phase transitions. The PGMA homopolymer is amorphous, and it shows a glass transition below 100°C. Homopolymer PAzoMA is known to exhibit a nematic and smectic A phase.[35] The endothermal peaks of the phase transitions related to the smectic-to-nematic transition temperature (T_{SN}) and the nematic-to-isotropic transition temperature (T_{NI}) on heating to the isotropic phase and the exothermic peaks of the phase transitions related to the isotropic-to-nematic transition temperature (T_{IN}) and the nematic-to-smectic transition temperature (T_{NS}) on cooling from the isotropic phase can be shown on the DSC curves. And, in addition, these phase transitions are reversible. More information can be obtained from the investigation on the phase transitions of PAzoMA block in PGMA-*b*-PAzoMA block copolymers, which is helpful to understand the relationship between structures and properties. Therefore, more attention is played to the thermal properties of the PAzoMA block in the block copolymer. Figure 4 reports the DSC curves of the second heating and first cooling scans of all the PGMA-*b*-PAzoMA diblock copolymers together with $PGMA_{65}$ and $PAzoMA_{60}$ homopolymers, the transition temperatures and the relative enthalpy changes are also summarized in Table II. Two series block copolymers, $PGMA_{42}$-*b*-$PAzoMA_n$ (n = 22, 39, and 63) and $PGMA_{65}$-*b*-$PAzoMA_m$ (m = 28, 38, and 67) were prepared to study the liquid crystal properties of PGMA-*b*-PAzoMA diblock copolymers. In Figure 4 and Table II, $PGMA_{65}$ homopolymer exhibits only a glass transition at 66.5°C and PGMA-*b*-PAzoMA diblock copolymers as well as the $PAzoMA_{60}$ homopolymer exhibit a glass transition, smectic, and nematic phase transitions on the second heating scan. For the $PGMA_{42}$-*b*-$PAzoMA_n$ (n = 22, 39, and 63) series, with increasing the molecular weight of block copolymers from 1.15×10^4 to 2.05×10^4 g mol^{-1} and the PAzoMA segment weight fraction from 60% to 81%, Tg, T_{SN}, T_{NI}, T_{IN}, and T_{NS} increase from 71.3 to 72.1°C, from 88.6

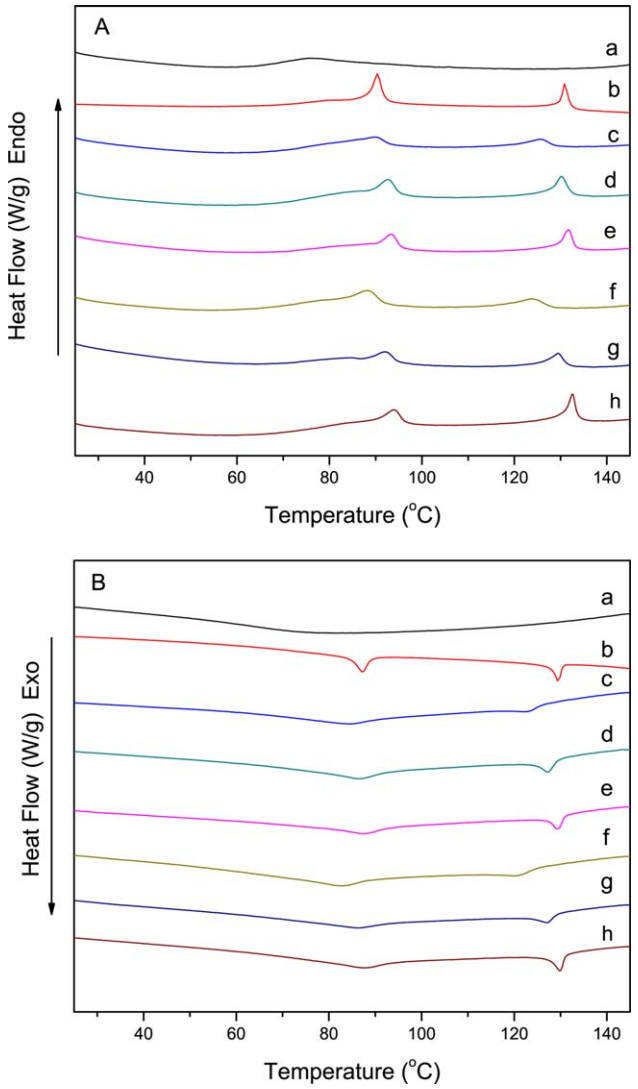

Figure 4. (A) The second heating and (B) the first cooling DSC curves of (a) $PGMA_{65}$, (b) $PAzoMA_{60}$, (c) $PGMA_{42}$-*b*-$PAzoMA_{22}$, (d) $PGMA_{42}$-*b*-$PAzoMA_{39}$, (e) $PGMA_{42}$-*b*-$PAzoMA_{63}$, (f) $PGMA_{65}$-*b*-$PAzoMA_{28}$, (g) $PGMA_{65}$-*b*-$PAzoMA_{38}$, and (h) $PGMA_{65}$-*b*-$PAzoMA_{67}$. [Color figure can be viewed in the online issue, which is available at wileyonlinelibrary.com.]

Table II. Thermal Transition Data of the Synthesized Polymers

Polymer	Phase transitions temperature (°C)[a]					Enthalpies (J/g)[b]			
	T_g	T_{SN}	T_{NI}	T_{IN}	T_{NS}	ΔH_{SN}	ΔH_{NI}	ΔH_{IN}	ΔH_{NS}
$PGMA_{42}$	–	–	–	–	–	–	–	–	–
$PGMA_{65}$	66.5	–	–	–	–	–	–	–	–
$PAzoMA_{60}$	77.8	92.1	131.5	130.1	87.4	3.21	2.87	−2.73	−3.17
$PGMA_{42}$-*b*-$PAzoMA_{22}$	71.3	88.6	124.8	123.1	84.5	0.75 (1.25)	0.55 (0.92)	−0.64 (−1.07)	−0.76 (−1.27)
$PGMA_{42}$-*b*-$PAzoMA_{39}$	72.1	92.1	129.6	127.2	86.5	1.23 (1.71)	0.72 (1.00)	−0.89 (−1.24)	−0.96 (−133)
$PGMA_{42}$-*b*-$PAzoMA_{63}$	72.9	92.7	131.1	129.6	87.7	1.47 (1.81)	1.04 (1.28)	−1.02 (−1.26)	−1.36 (−1.68)
$PGMA_{65}$-*b*-$PAzoMA_{28}$	67.3	87.5	123.2	120.7	82.5	0.88 (1.42)	0.73 (1.18)	−0.77 (−1.24)	−1.26 (−2.03)
$PGMA_{65}$-*b*-$PAzoMA_{38}$	70.0	91.5	128.9	127.2	86.2	1.22 (1.82)	0.78 (1.16)	−0.77 (−1.15)	−1.59 (−2.37)
$PGMA_{65}$-*b*-$PAzoMA_{67}$	72.6	94.4	132.0	131.4	87.6	1.70 (2.30)	1.39 (1.88)	−1.25 (−1.69)	−1.81 (−2.45)

[a] T_g, T_{SN}, T_{NI}, T_{IN}, and T_{NS} were designated to the glass transition temperature, the smectic-to-nematic transition temperature, the nematic-to-isotropic transition temperature, the isotropic-to-nematic transition temperature, and the nematic-to-smectic transition temperature, respectively, and the corresponding enthalpies were denoted as ΔH_{SN}, ΔH_{NI}, ΔH_{IN}, and ΔH_{NS}. T_g, T_{SN}, T_{NI}, ΔH_{SN}, and ΔH_{NI} were determined by DSC on the second heating process, and T_{IN}, T_{NS}, ΔH_{IN}, and ΔH_N were determined by DSC on the first cooling process.

[b] The normalized enthalpies shown in parentheses were calculated from the weight fraction of PAzoMA block and the corresponding enthalpies of the block copolymers according to the equation: the normalized enthalpy = the enthalpy/f_{PAzoMA}

to 92.7°C, from 124.8 to 131.1°C, from 123.1 to 129.4°C, and from 84.5 to 87.7°C, respectively. Meanwhile, the corresponding enthalpies also increase with increasing the PAzoMA block molecular weights (Table II). The phenomenon is similar to the $PGMA_{65}$-*b*-$PAzoMA_m$ (m = 28, 38, and 67) series which have longer PGMA block. This change trend coincides with other Azo-SCLCPs reported before.[35–37] It is indicated that the PGMA-*b*-PAzoMA diblock copolymers mainly displayed the liquid crystal transitions of the PAzoMA segment. The phenomena might be due to the microphase-separation between the coil PGMA block and the rod PAzoMA block. The formed microphase-separated nanostructures were also demonstrated with the AFM images of the diblock copolymer $PGMA_{65}$-*b*-$PAzoMA_{67}$, as shown in Figure 5. The dotted nanostructures were clearly observed in $PGMA_{65}$-*b*-$PAzoMA_{67}$ annealed film [Figure 5(A)]. In microphase-separated nanostructures of the diblock copolymer thin films, amorphous PGMA formed the isotropic domains and the liquid crystal PAzoMA formed the mesogen domains. This may imply that PGMA block is partially compatible with PAzoMA block in the microphase-separated nanostructures of the annealed films and the cross-linking reaction enhanced the incompatibility between the two blocks which is benefit to the formation of the microphase separation. As to $PGMA_{42}$-*b*-$PAzoMA_{67}$ with lower PGMA weight fraction, the observed microphase separation became a little fuzzy even for the occurrence of cross-linking reaction (Supporting Information Figure 1S). The annealed films and cross-linked films were prepared under vacuum so that the solvent effect was minimized and the microphase-separation was mainly affected by the relative length of the two blocks.

POM was used to observe the textures of the block copolymers. The solid samples were first heating to a temperature higher than T_{NI} (~150°C) and then subsequent cooling down to room temperature. The images were taken during the cooling progress. The texture of a representative example $PGMA_{65}$-*b*-$PAzoMA_{67}$ at 86°C is shown in Figure 6. A typical gritty texture could be observed for the smectic phase in the thermal treatment and remained unchanged during the cooling process. The similar gritty textures were also found in other samples, such as $PGMA_{42}$-*b*-$PAzoMA_{22}$ and $PGMA_{42}$-*b*-$PAzoMA_{63}$ (Supporting Information Figure 2S).

Photo-Responsive Behavior

Azobenzene-containing polymers are of great interest in their photo-responsive properties due to the reversible *trans–cis* isomerization of the azobenzene chromophores caused by photo irradiation.[2438–40] The reversible isomerization of the azobenzene chromophores changes remarkably according to both external conditions and internal structures. To explore photo-responsive properties of the synthesized block copolymers PGMA-*b*-PAzoMA, we first investigated the photoisomerization processes of PGMA-*b*-PAzoMA diblock copolymers as well as $PAzoMA_{60}$ homopolymer in $CHCl_3$ dilute solution under the irradiation of 365 nm UV light and 450 nm visible light. Figure 7 shows the photoisomerization processes of the representative sample $PGMA_{65}$-*b*-$PAzoMA_{67}$ in $CHCl_3$ solution with the irradiation of 365 nm light (A) and 450 nm light (B), respectively. The absorption peak at 359 nm attributed to the π–π^* transition of *trans* azobenzene isomers strongly decreased and the intensity of the absorption peak at 447 nm which is assigned to the n–π^* transition of the *cis* azobenzene isomers slightly increased with successive 365 nm UV light irradiation, which indicated the *trans–cis* isomerization of the azobenzene moieties of PAzoMA block. Meanwhile, the kinetic rates of $PAzoMA_{60}$ homopolymer and PGMA-*b*-PAzoMA diblock copolymers were further studied. Their photoisomerization kinetics curves are plotted in Figure 8 and the first-order kinetic rates for their *trans–cis* photoisomerization can be obtained. The kinetic rate ($k_{t\text{-}c}$) is calculated by the following equation[41]:

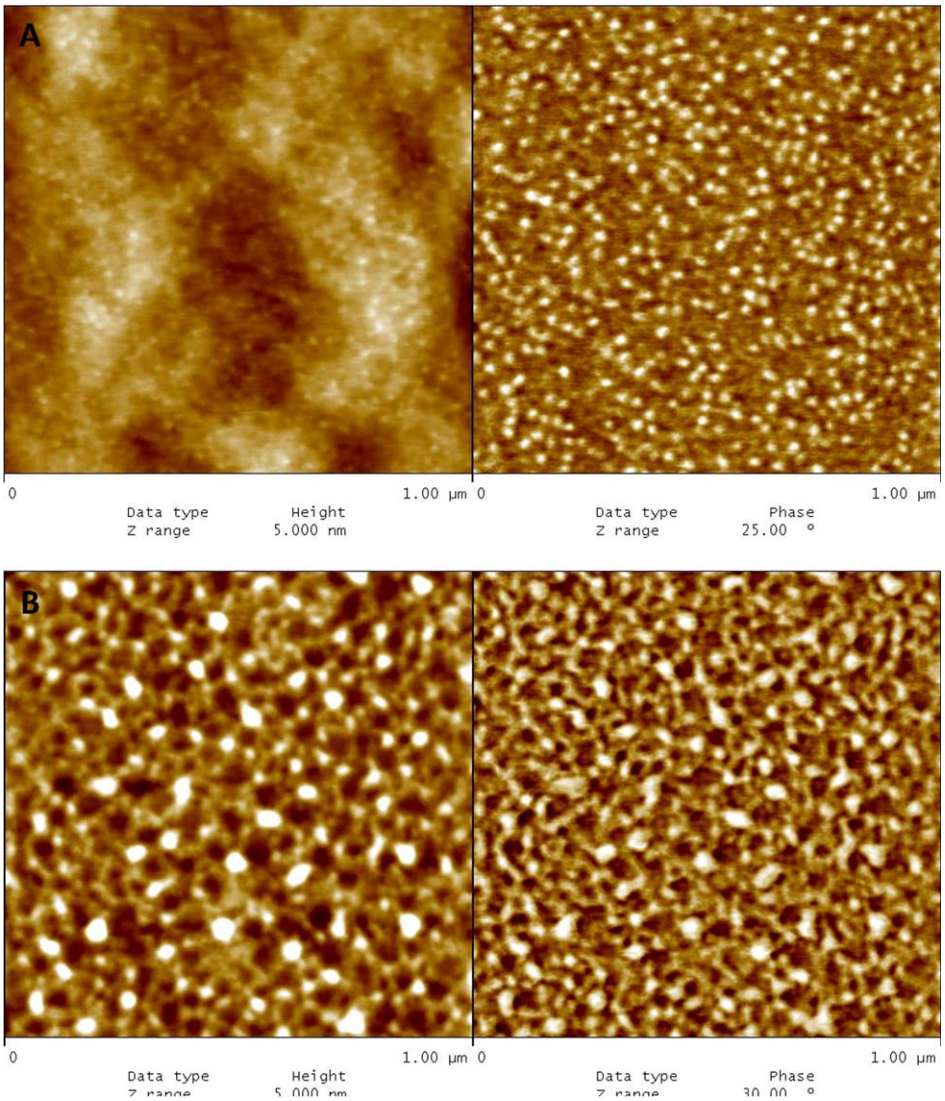

Figure 5. The AFM images of $PGMA_{65}$-*b*-$PAzoMA_{67}$ in (A) annealed film and (B) crosslinked film. [Color figure can be viewed in the online issue, which is available at wileyonlinelibrary.com.]

$$\ln \frac{(A_{eq}-A_t)}{(A_{eq}-A_0)} = -k_{t-c}t \quad (1)$$

where A_0, A_t, and A_{eq} are the initial absorbance, the absorbance at time *t*, and the absorbance at the photostationary state at 359 nm in the UV–vis spectra, respectively. The photoisomerization rate constants (k_{t-c}) of $PGMA_{65}$-*b*-$PAzoMA_n$ (n = 28, 38, and 67) series were 0.040, 0.034, and 0.032 s^{-1}, respectively, which decreased with increasing the length of the PAzoMA block while keeping the length of PGMA block unchanged. The molecular weights of the diblock copolymers promoted the chain winding factor and limited the free volume for the *trans–cis* photoisomerization of azobenzene chromophores in PAzoMA segment. As to $PGMA_{42}$-b-$PAzoMA_n$ (n = 22, 39, and 63) series, a similar result was also obtained (Supporting Information Figure 3S). The k_{t-c} values of $PAzoMA_{60}$ homopolymer, $PGMA_{42}$-*b*-$PAzoMA_{63}$, and $PGMA_{65}$-*b*-$PAzoMA_{67}$ diblock copolymers which have similar molecular weights of PAzoMA were 0.056, 0.038, and 0.032 s^{-1} [Figure 8(B)], respectively. It was found

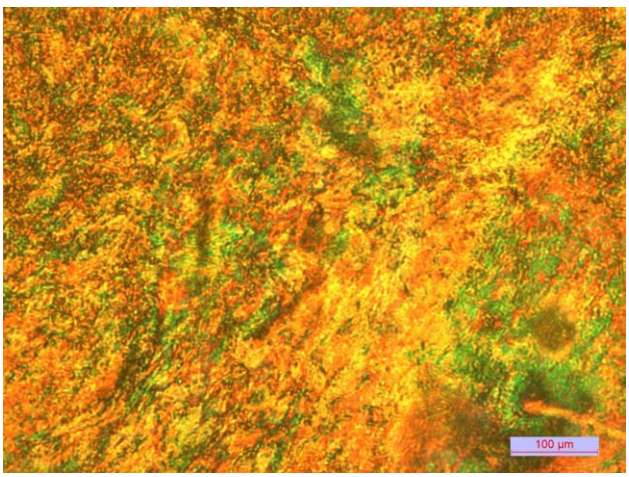

Figure 6. Polarized optical micrograph of $PGMA_{65}$-*b*-$PAzoMA_{67}$ at 86°C. [Color figure can be viewed in the online issue, which is available at wileyonlinelibrary.com.]

Applied Polymer SCIENCE

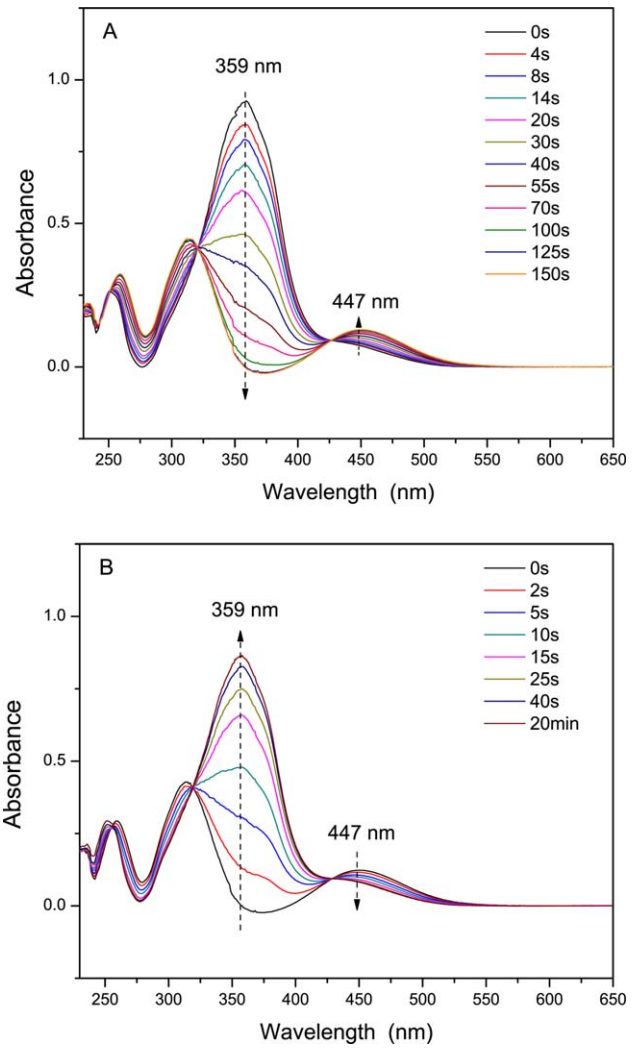

Figure 7. The photoisomerization progress of $PGMA_{65}$-*b*-$PAzoMA_{67}$ in $CHCl_3$ solution with the irradiation of (A) 365 nm light and (B) 450 nm light, respectively. [Color figure can be viewed in the online issue, which is available at wileyonlinelibrary.com.]

that the k_{t-c} values decreased with increasing the length of the PGMA block. The results suggested that the introducing of the PGMA block into PAzoMA chain reduced the rate of *trans–cis* photoisomerization of azobenzene chromophores.

On the other hand, we also explored the photoisomerization of azobenzene chromophores of the synthesized block copolymers in film. $PGMA_{65}$-*b*-$PAzoMA_{67}$ was chosen as a representative sample to prepare the films. $PAzoMA_{60}$ homopolymer was used as a reference. Figure 9 displays the photoisomerization processes of the as-coated film (A and B), the annealed film (C and D), and the cross-linked film of $PGMA_{65}$-*b*-$PAzoMA_{67}$ (E and F) with the irradiation of 365 nm light (A, C, and E) and 450 nm light (B, D, and F), respectively. The as-coated film and annealed film of homopolymer $PAzoMA_{60}$ film were used as a reference (Supporting Information Figure 4S). In solid thin films, the segmental mobility of the polymer was restrained and the azo side groups tended to associate with each other than that in dilute solution. Before the UV irradiation, the as-coated film, the annealed film, and the cross-linked film of the block copolymer $PGMA_{65}$-*b*-$PAzoMA_{67}$ exhibit a similar broad absorption band with two main absorption point fixed at 359 nm for the non-association and 344 nm (blue-shifted) for H-aggregation (face-to-face) as well as a shoulder (red-shifted) at about 380 nm for J-aggregation (head-to-head) of azobenzene chromophores [Figure 9 A, C, and E)].[42,43] With the successive irradiation of 365 nm light, the three films display the similar photochemical process with the absorption strength of the *trans* azobenzene isomers around 359 nm decreased successively, which indicated that the azobenzene chromophores in the three films were located at a similar aggregation state. These photoisomerization were similar with those of homopolymer $PAzoMA_{60}$ films (Supporting Information Figure 4S). That is to say, the azobenzene chromophores located in the PAzoMA micro-domains formed by the microphase-separation in the

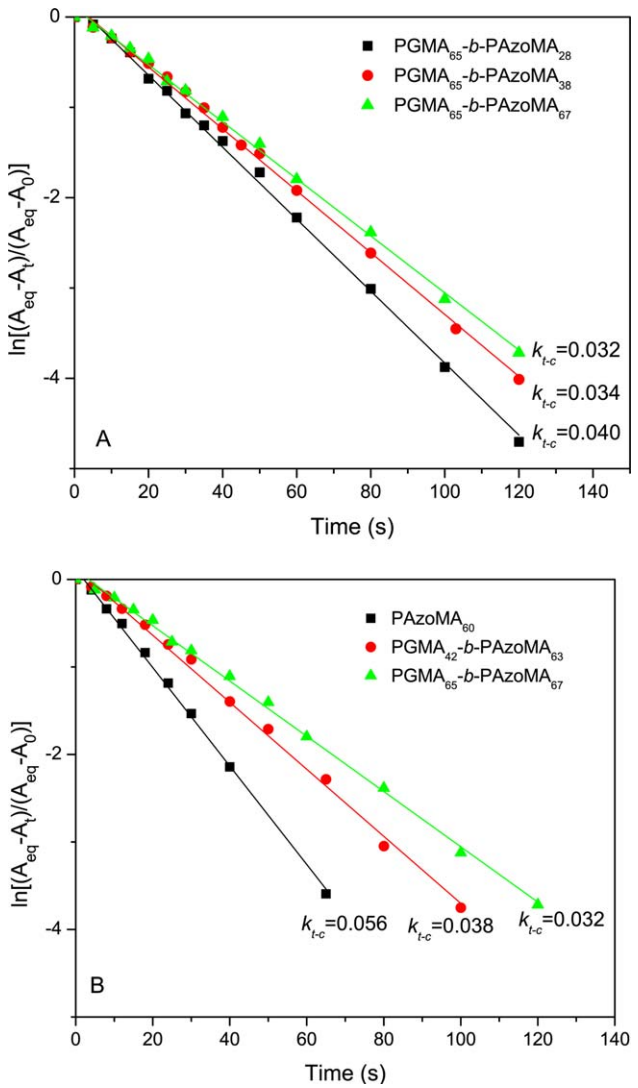

Figure 8. First-order plots for *trans–cis* isomerization of $PGMA_{65}$-*b*-$PAzoMA_m$ (m = 28, 38, and 67) series (A) and $PAzoMA_{60}$ homopolymer, $PGMA_{42}$-*b*-$PAzoMA_{63}$ and $PGMA_{65}$-*b*-$PAzoMA_{67}$ diblock copolymers (B) in $CHCl_3$. [Color figure can be viewed in the online issue, which is available at wileyonlinelibrary.com.]

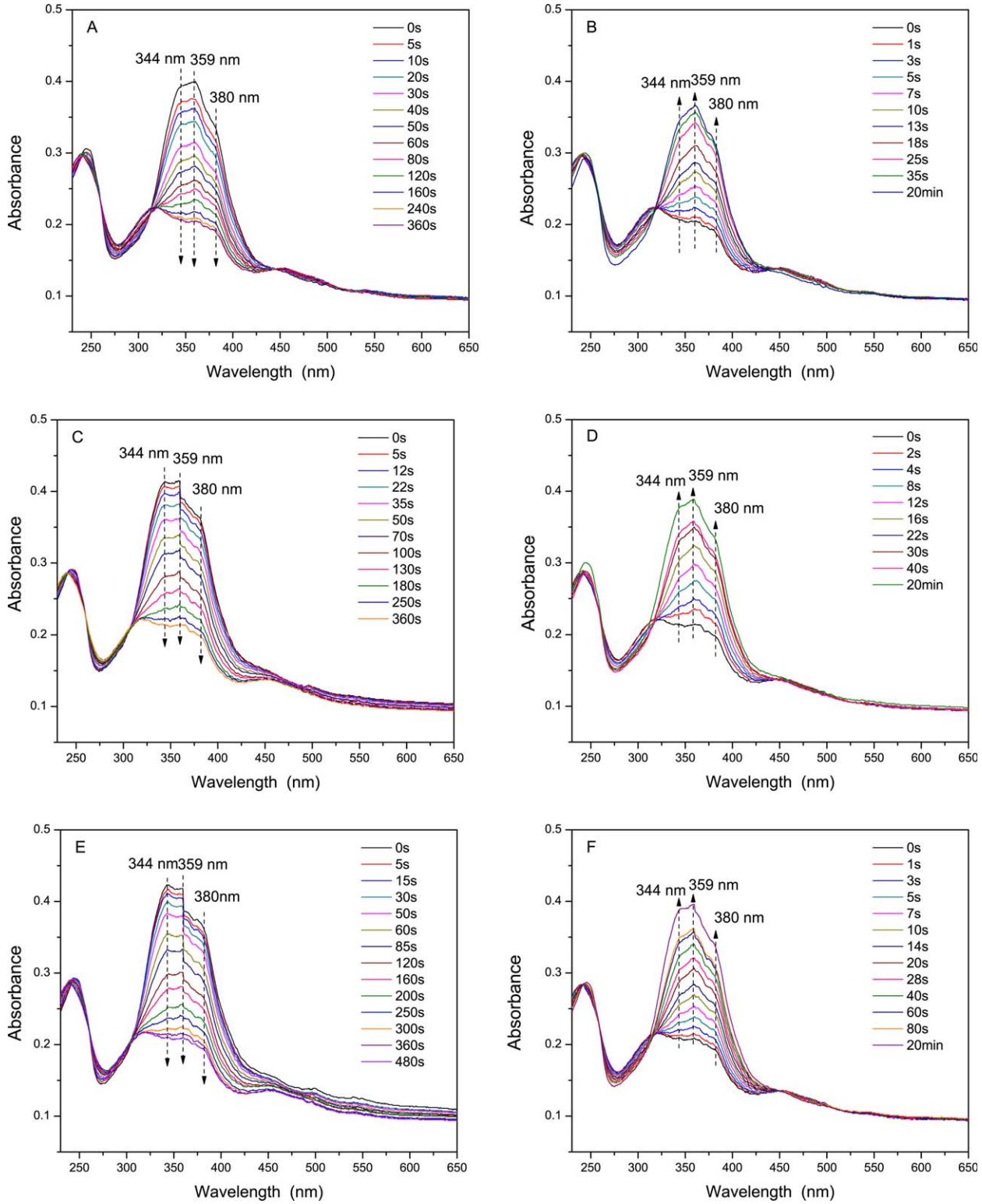

Figure 9. The photoisomerization processes of (A,B) the as-coated film, (C,D) the annealed film, and (E,F) the crosslinked film of $PGMA_{65}$-*b*-$PAzoMA_{67}$ with the irradiation of 365 nm light (A,C,E) and 450 nm light (B,D, F), respectively. [Color figure can be viewed in the online issue, which is available at wileyonlinelibrary.com.]

$PGMA_{65}$-*b*-$PAzoMA_{67}$ diblock copolymer [Figure. 5(A,B)] showed the similar aggregation state as those of homopolymer PAzoMA. In addition, the *cis–trans* back reaction progress of the as-coated, annealed, and cross-linked films [Figure 9 (B, E, and F)] also exhibit a similar photoisomerization process with successive increase of the absorption strength of the broad

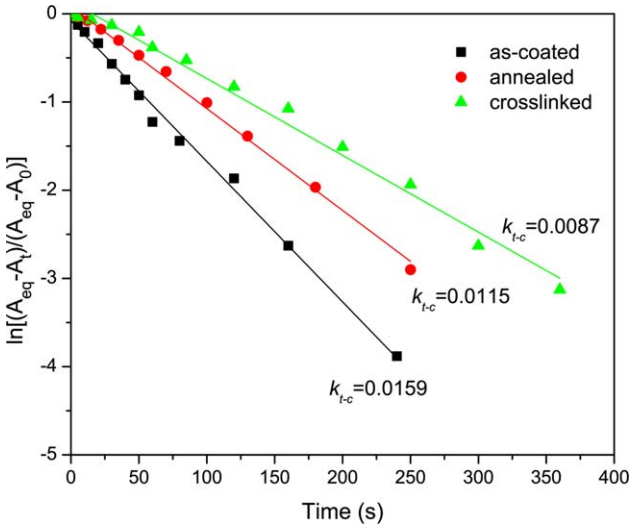

Figure 10. First-order plots for *trans–cis* isomerization of $PGMA_{65}$-*b*-$PAzoMA_{67}$ in the as-coated, annealed, and cross-linked film. [Color figure can be viewed in the online issue, which is available at wileyonlinelibrary.com.]

absorption band around 359 nm, in which the absorbance at 359 nm ascribed to the non-association is obviously higher than that of a blue-shifted shoulder at about 344 nm ascribed to the H-aggregation compared to the initial films without UV irradiation. It is indicated that the H-aggregation of azobenzene chromophores formed were broken by the photochemical process and the reorganization of the azobenzene chromophores to the H-aggregation did not totally recover due to absence of sufficient free volume in solid film.[36,44] However, in the cross-linked film, the chain mobility was greatly reduced and cross-linked PGMA domains hindered the formation of larger PAzoMA mesogen domains, so that the sufficient free volume for the photochemical transition of azobenzene side groups was smaller than the annealed film. Therefore, the isomerization progress took more time than that of the annealed film. The results confirm that the steric hindrance around azobenzene chromophores play an important role in the photo-responsive behavior. To better illustrate the phenomenon, we performed a similar kinetic study on the *trans–cis* photoisomerization of azobenzene chromophores in the as-coated, annealed, and cross-linked films of $PGMA_{65}$-*b*-$PAzoMA_{67}$ diblock copolymer upon irradiation using 365 nm light. Their photoisomerization kinetics curves are plotted in Figure 10 and the first-order kinetic rates of their *trans–cis* photoisomerization for the as-coated, annealed, and cross-linked films were 0.0159, 0.0115, and 0.0087 s^{-1}, respectively. It was clearly found that the micro-domain structures and cross-linking structures severely suppressed the photoisomerization rate of azobenzene chromophores. These results may provide guidelines for the design of effective photo-responsive anisotropic materials.

CONCLUSION

Well-defined azobenzene-containing side-chain liquid crystalline diblock copolymers PGMA-*b*-PAzoMA were successfully synthesized via RAFT polymerization. The chemical structures were proved by ^{1}H NMR, IR, and GPC. The PGMA-*b*-PAzoMA diblock copolymers exhibited a smectic and nematic liquid crystalline phase over a relatively wide temperature range. The microphase-separated structures formed by annealing and cross-linking between the PGMA block and the PAzoMA block can be observed from the AFM images of block copolymers. Introducing PGMA into PAzoMA chain and increasing the length of PAzoMA block can lower the rate of *trans–cis* photoisomerization of azobenzene chromophores in solution. In solid film, although the as-coated film, annealed film, and cross-linked films of diblock copolymers PGMA-*b*-PAzoMA diblock copolymers exhibit similar spectral shapes, a different photoisomerization rate change between the as-coated, annealed, and cross-linked block copolymer films is obvious, indicating the effect of the PGMA micro-domain on the photoisomerization behavior.

ACKNOWLEDGMENTS

We acknowledge the financial support from the National Natural Science Foundation of China (21174038 and 51103044). Support from Projects of Shanghai Municipality (12JC1403102), the Shanghai Key Laboratory of Advanced Polymer Materials (ZD20100101), and the Large Instruments Open Foundation of East China Normal University are also appreciated.

REFERENCES

1. Natansohn, A.; Rochon, P. *Chem. Rev.* **2002**, *102*, 4139.
2. Ichimura, K. *Chem. Rev.* **2000**, *100*, 1847.
3. Zhao, Y.; He, J. *Soft Matter* **2009**, *5*, 2686.
4. Yang, P. C.; Wang, Y. H.; Wu, H. *J. Appl. Polym. Sci.* **2012**, *124*, 4193.
5. Kadota, S.; Aoki, K.; Nagano, S.; Seki, T. *J. Am. Chem. Soc.* **2005**, *127*, 8266.
6. Yu, H.; Iyoda, T.; Ikeda, T. *J. Am. Chem. Soc.* **2006**, *128*, 11010.
7. Yu, H.; Asaoka, S.; Shishido, A.; Iyoda, T.; Ikeda, T. *Small* **2007**, *3*, 768.
8. Cui, L.; Zhao, Y.; Yavrian, A.; Galstian, T. *Macromolecules* **2003**, *36*, 8246.
9. Deng, W.; Albouy, P.-A.; Lacaze, E.; Keller, P.; Wang, X.; Li, M.-H. *Macromolecules* **2008**, *41*, 2459.
10. Forcén, P.; Oriol, L.; Sánchez, C.; Alcalá, R.; Hvilsted, S.; Jankova, K.; Loos, J. *J. Polym. Sci., Part A: Polym. Chem.* **2007**, *45*, 1899.
11. Wang, G.; Tong, X.; Zhao, Y. *Macromolecules* **2004**, *37*, 8911.
12. Moriya, K.; Seki, T.; Nakagawa, M.; Mao, G.; Ober, C. K. *Macromol. Rapid Commun.* **2000**, *21*, 1309.
13. Liu, J. H.; Chiu, Y. H. *J. Polym. Sci., Part A: Polym. Chem.* **2010**, *48*, 1142.
14. He, X.; Sun, W.; Yan, D.; Xie, M.; Zhang, Y. *J. Polym. Sci., Part A: Polym. Chem.* **2008**, *46*, 4442.
15. Zhao, Y.; Tong, X.; Zhao, Y. *Macromol. Rapid Commun.* **2010**, *31*, 986.
16. Berges, C.; Gimeno, N.; Oriol, L.; Piñol, M.; Forcén, P.; Sánchez, C.; Alcalá, R. *Eur. Polym. J.* **2012**, *48*, 613.

17. He, X.; Sun, W.; Yan, D.; Liang, L. *Eur. Polym. J.* **2008**, *44*, 42.
18. Boyer, C.; Bulmus, V.; Davis, T. P.; Ladmiral, V.; Liu, J.; Perrier, S. B. *Chem. Rev.* **2009**, *109*, 5402.
19. Su, W.; Han, K.; Luo, Y.; Wang, Z.; Li, Y.; Zhang, Q. *Macromol. Chem. Phys.* **2007**, *208*, 955.
20. Su, W.; Luo, Y.; Yan, Q.; Wu, S.; Han, K.; Zhang, Q.; Gu, Y.; Li, Y. *Macromol. Rapid Commun.* **2007**, *28*, 1251.
21. Su, W.; Zhao, H.; Wang, Z.; Li, Y.; Zhang, Q. *Eur. Polym. J.* **2007**, *43*, 657.
22. Xu, J.; Zhang, W.; Zhou, N.; Zhu, J.; Cheng, Z.; Xu, Y.; Zhu, X. *J. Polym. Sci., Part A: Polym. Chem.* **2008**, *46*, 5652.
23. Yu, L.; Zhang, Z.; Chen, X.; Zhang, W.; Wu, J.; Cheng, Z.; Zhu, J.; Zhu, X. *J. Polym. Sci., Part A: Polym. Chem.* **2008**, *46*, 682.
24. Zhao, Y.; Qi, B.; Tong, X.; Zhao, Y. *Macromolecules* **2008**, *41*, 3823.
25. Zhao, Y.; Tremblay, L.; Zhao, Y. *J. Polym. Sci., Part A: Polym. Chem.* **2010**, *48*, 4055.
26. Ding, H.; Wang, Z.; Sheng, L.; Song, G. *Polym. Eng. Sci.* **2011**, *51*, 1662.
27. Li, Y.; Zhou, N.; Zhang, W.; Zhang, F.; Zhu, J.; Zhang, Z.; Cheng, Z.; Tu, Y.; Zhu, X. *J. Polym. Sci., Part A: Polym. Chem.* **2011**, *49*, 4911.
28. Yan, B.; Tong, X.; Ayotte, P.; Zhao, Y. *Soft Matter* **2011**, *7*, 10001.
29. Ueki, T.; Nakamura, Y.; Lodge, T. P.; Watanabe, M. *Macromolecules* **2012**, *45*, 7566.
30. Zhu, Y.; Zhou, Y.; Chen, Z.; Lin, R.; Wang, X. *Polymer* **2012**, *53*, 3566.
31. Xie, H. L.; Liu, Y. X.; Zhong, G. Q.; Zhang, H. L.; Chen, E.-Q.; Zhou, Q.-F. *Macromolecules* **2009**, *42*, 8774.
32. Stewart, D.; Imrie, C. T. *Polymer* **1996**, *37*, 3419.
33. Perrier, S.; Barner-Kowollik, C.; Quinn, J. F.; Vana, P.; Davis, T. P. *Macromolecules* **2002**, *35*, 8300.
34. Cheng, Z.; Zhu, X.; Fu, G. D.; Kang, E. T.; Neoh, K. G. *Macromolecules* **2005**, *38*, 7187.
35. Han, D.; Tong, X.; Zhao, Y.; Galstian, T.; Zhao, Y. *Macromolecules* **2010**, *43*, 3664.
36. Tian, Y.; Watanabe, K.; Kong, X.; Abe, J.; Iyoda, T. *Macromolecules* **2002**, *35*, 3739.
37. He, X.; Zhang, H.; Yan, D.; Wang, X. J. *Polym. Sci., Part A: Polym. Chem.* **2003**, *41*, 2854.
38. Yu, B.; Jiang, X.; Wang, R.; Yin, J. *Macromolecules* **2010**, *43*, 10457.
39. Huang, C.-F.; Chen, W.; Russell, T. P.; Balazs, A. C.; Chang, F.-C.; Matyjaszewski, K. *Macromol. Chem. Phys.* **2009**, *210*, 1484.
40. Tang, X.; Gao, L.; Fan, X.; Liang, X.; Zhou, Q. *Macromol. Chem. Phys.* **2009**, *210*, 1556.
41. Zielińska, S.; Larkowska, M.; Kucharski, S. *Dyes Pigm.* **2012**, *92*, 1018.
42. Tong, X.; Cui, L.; Zhao, Y. *Macromolecules* **2004**, *37*, 3101.
43. Menzel, H.; Weichart, B.; Schmidt, A.; Paul, S.; Knoll, W.; Stumpe, J.; Fischer, T. *Langmuir* **1994**, *10*, 1926.
44. Fernández, R.; Zalakain, I.; Ramos, J. A.; Martin, L.; Mondragon, I. *Eur. Polym. J.* **2011**, *47*, 1176.